PAPER • OPEN ACCESS

Laser photodetachment of radioactive $^{128}I^{-}$

View the article online for updates and enhancements.

Related content

- Determination of the electron affinity of iodine
  D Hanstorp and M Gustafsson

- Ion beam production and study of radioactive isotopes with the laser ion source at ISOLDE
  Valentin Fedosseev, Katerina Chrysalidis, Thomas Day Goodacre et al.

- A secondary emission detector capable of preventing detection of the photoelectric effect induced by pulsed lasers
  D Hanstorp

Laser photodetachment of radioactive ^{128}I$^-$

Sebastian Rothe[1,2,3] , **Julia Sundberg**[1,2], **Jakob Welander**[2],
Katerina Chrysalidis[1,4], **Thomas Day Goodacre**[1,3],
Valentin Fedosseev[1], **Spyridon Fiotakis**[1], **Oliver Forstner**[5],
Reinhard Heinke[4], **Karl Johnston**[1], **Tobias Kron**[4],
Ulli Köster[6], **Yuan Liu**[7] , **Bruce Marsh**[1],
Annie Ringvall-Moberg[1,2], **Ralf Erik Rossel**[1,4],
Christoph Seiffert[1], **Dominik Studer**[4], **Klaus Wendt**[4] **and
Dag Hanstorp**[2]

[1] CERN, Geneva, Switzerland
[2] Department of Physics, University of Gothenburg, Gothenburg, Sweden
[3] School of Physics and Astronomy, The University of Manchester, Manchester, United Kingdom
[4] Institut für Physik, Johannes Gutenberg-Universität, Mainz, Germany
[5] Institut für Optik und Quantenelektronik, Friedrich-Schiller-Universität, Jena, Germany
[6] Institut Laue-Langevin (ILL), Grenoble, France
[7] Physics Division, Oak Ridge National Laboratory (ORNL), Oak Ridge, Tennessee, United States of America

E-mail: sebastian.rothe@cern.ch

CrossMark

Abstract
The first experimental investigation of the electron affinity (EA) of a radio-active isotope has been conducted at the CERN-ISOLDE radioactive ion beam facility. The EA of the radioactive iodine isotope ^{128}I ($t_{1/2} = 25$ min) was determined to be 3.059 052(38) eV. The experiment was conducted using the newly developed Gothenburg ANion Detector for Affinity measurements by Laser PHotodetachment (GANDALPH) apparatus, connected to a CERN-ISOLDE experimental beamline. ^{128}I was produced in fission induced by 1.4 GeV protons striking a thorium/tantalum foil target and then extracted as singly charged negative ions at a beam energy of 20 keV. Laser photo-detachment of the fast ion beam was performed in a collinear geometry inside the GANDALPH chamber. Neutral atoms produced in the photodetachment

process were detected by allowing them to impinge on a glass surface, creating secondary electrons which were then detected using a channel electron multiplier. The photon energy of the laser was tuned across the threshold of the photodetachment process and the detachment threshold data were fitted to a Wigner law function in order to extract the EA. This first successful demonstration of photodetachment at an isotope separator on line facility opens up the opportunity for future studies of the fundamental properties of negatively charged radioactive isotopes such as the EA of astatine and polonium.

Keywords: ISOLDE, electron affinity, iodine, photodetachment

(Some figures may appear in colour only in the online journal)

1. Introduction

Negative ions are unique quantum systems. The lack of a long-range Coulomb force acting on the valence electron gives them binding energies that are about an order of magnitude smaller than in neutral systems [1]. Furthermore, the short-range binding force can support only a few, if any, bound excited states of usually the same parity, and almost all transitions within negative ions are correspondingly optically forbidden [2]. Hence, traditional spectroscopic methods, which are used to identify and to determine the structure of atoms and positive ions, cannot be applied to negative ions. These weakly bound systems are abundant in many environments such as the solar atmosphere [3], the interstellar medium [4] and in plasmas [5]. However, their presence is often extremely difficult to detect as a consequence of the scarcity of radiative transitions between bound states. Furthermore, their unique properties provide valuable tools in many different applications, such as accelerator-based mass spectrometry [6] and fusion research [7].

The lack of a long-range Coulomb force causes the inter-electronic interaction to have an enhanced importance. As a consequence, the independent particle model, which adequately describes the atomic structure under normal conditions, breaks down. Experimental studies of negative ions can thus serve as a useful probe of electron correlations and hence be used to test theoretical models that go beyond the independent particle approximation [2]. A consequence of the lack of bound excited states is that, with very few exceptions, the only atomic parameter that can be determined with high accuracy for a negative ion is the electron affinity (EA) of the parent atom, i.e. the energy released when an additional electron is attached to a neutral atom forming a negative ion. Today, the EA of most elements that form stable negative ions [1] have been experimentally determined. The most precise measurements have been made using either the photodetachment microscope technique [8] or the laser photodetachment threshold (LPT) method [9]. For the elements lacking stable isotopes, however, there are so far no experimental studies of their EAs.

One particularly interesting radioactive element is astatine (At, $Z = 85$), which is among the rarest of the naturally occurring elements on Earth [10]. One of its longest-lived isotopes, ^{211}At (half-life $t_{1/2} = 7.2$ h), is a promising candidate as a radio-therapeutic agent for Targeted Alpha Therapy (TAT) in nuclear medicine [11, 12]. Here experimental values of fundamental atomic properties such as the ionization potential (IP) and the EA are required to benchmark quantum chemistry calculations [13–16]. The electronegativity of an element can be derived from the IP and EA [17], and it is a key factor to predict chemical properties of that element in compounds. The IP of At (9.317 51(8) eV) [18] was first measured experimentally
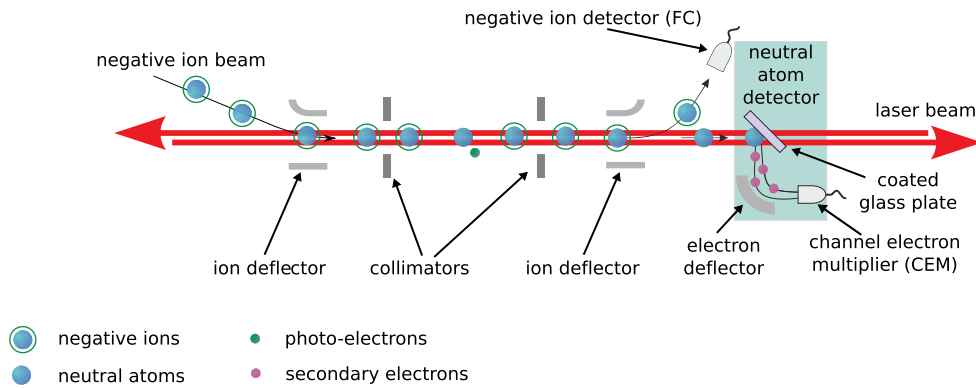
Figure 1. Schematic layout of the collinear laser photodetachment method. The beam of negative ions is overlapped with a laser beam, arranged in either a co- or counter-propagating geometry. The neutral atoms produced in the photodetachment process impinge on a coated glass substrate and create secondary electrons. These electrons are deflected 90° by means of an electrode where they are detected by a single channel electron multiplier. The remaining undetached ions are deflected towards a Faraday cup.

at ISOLDE [19] by resonance ionization spectroscopy of astatine isotopes produced using the isotope separator on line (ISOL) method [20].

As a milestone on the way towards measuring the EA of astatine we present here the first investigation of a radioactive negative ion: the measurement of the EA of ^{128}I ($t_{1/2} = 25$ min).

2. Methods

The experimental arrangement used for studying photodetachment of radioactive negative ions is shown in figure 1. A beam of negative ^{128}I ions was overlapped with a laser beam over a 50 cm long path inside the Gothenburg ANion Detector for Affinity measurements by Laser PHotodetachment (GANDALPH). The neutral atoms produced in the photodetachment process impinged on a coated glass surface where the resulting secondary electrons were detected using a single channel electron multiplier (CEM). The wavelength of the laser was tuned in such a way that the photon energy spanned the threshold for the photodetachment process, and the secondary electrons were collected as a function of photon energy. The analysis of the characteristic photodetachment threshold spectrum enabled the determination of the EA of ^{128}I.

2.1. Negative radioactive ion beam production at ISOLDE

ISOLDE [19] is a radioactive ion beam facility based at CERN where protons at an energy of 1.4 GeV from the proton synchrotron booster (PSB) impinge on a thick target in which they induce nuclear reactions. The reaction products are evaporated from the target matrix, ionized and mass-separated using dipole magnets. The magnetic field is adjusted in such a way that ions of a selected mass are delivered to the experiment.

In our experiment ^{128}I was produced in a thorium/tantalum foil target [21, 22] and ionized using an ISOLDE MK4 negative surface ion source [23, 24] to obtain singly charged

negative ions. The source comprises a LaB_6 pellet positioned at the end of the tubular transfer line. The work function of LaB_6 is ~2.7 eV. Upon contact with the surface of the pellet, iodine with an EA of ~3 eV, is negatively ionized with an efficiency close to unity. Isotopes of neighboring elements also produced in the target are suppressed by orders of magnitude in negative ion formation due to their significantly lower EAs. A sample of stable iodine ^{127}I was placed in a tantalum capillary (mass-marker) which was attached to the ion source in order to produce an iodine ion beam for tuning and reference measurements. The target and ion source unit was mounted on the front end of the ISOLDE General Purpose mass Separator (GPS). A voltage of 20 kV was supplied to the front end, accelerating the negative ions towards the grounded extraction electrode at the exit of the ion source.

The GANDALPH apparatus was connected to the low-mass beamline of the GPS (GLM), which is the closest suitable location to the Resonance Ionization Laser Ion Source (RILIS) laboratory providing the laser beam used in our experiment.

2.2. Laser system

The EA of stable iodine ^{127}I is 3.059 046 3(38) eV [25], which corresponds to the energy of photons at a wavelength of approximately 405 nm. In previous LPT experiments conducted at the GUNILLA setup [26] at the University of Gothenburg, 10 Hz repetition rate dye-lasers or OPO systems have been used [9, 27, 28] to measure the EAs of atomic systems. A pulse energy exceeding 10 mJ is typically achievable with this low repetition rate laser system. The titanium:sapphire laser (Ti:Sa) [29] available at the ISOLDE-RILIS laser setup [30] however, operates at a repetition rate of 10 kHz, with a typical pulse energy of <0.1 mJ at 405 nm (second harmonic) and a spectral line-width of the order of 10 GHz (fundamental laser wavelength). Therefore, in a preparatory experiment, the suitability of a CERN-Ti:Sa laser was tested during an experimental test at the GUNILLA facility. The tests confirmed the compatibility of the LPT technique with this alternative laser system. The lower pulse energy of the Ti:Sa laser is well compensated by the 1000-fold increased duty-cycle factor due to the higher repetition rate. Furthermore, a lower photon intensity is favorable to prevent saturation effects due to dead-time of the CEM and the detector electronics. In addition, it was shown that the neutral particle detector [31] used in those studies can be operated at a 10 kHz repetition rate.

A new optical beam path from the RILIS setup to the GLM beamline was established for the present experiment. The laser beam was collimated to a size of 6 mm in diameter by a telescope located just after the second-harmonic generation unit. The maximum laser power, measured after passing through the GANDALPH beamline and the neutral atom detector glass plate was 450 mW. The fundamental laser wavelength was measured with a fiber-coupled wavelength meter (Highfinesse/Angstrom WS7).

2.3. GANDALPH

GANDALPH has been developed and manufactured at the University of Gothenburg and assembled at CERN-ISOLDE. It is designed to be coupled to the ISOLDE GLM experimental beamline. The central part of GANDALPH is a 50 cm long photon/ion interaction region, defined by two 6.35 mm diameter apertures within which both the ion beam and the laser beam can be overlapped, either in a co- or counter-propagating geometry. For this purpose the ion beam is deflected by 10° into the path of the laser beam by a pair of electrostatic deflection plates. After passing through the interaction region, the remaining ions are deflected by a second pair of electrostatic plates and guided into a Faraday cup.
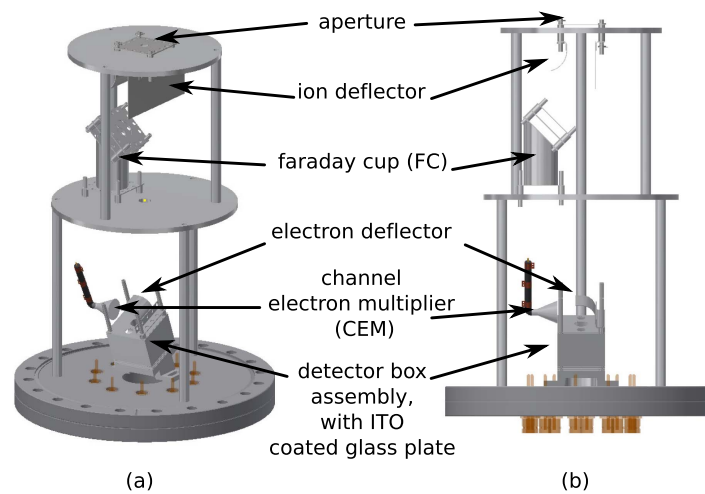
Figure 2. 3D drawing of the neutral particle detector setup. Visible from top to bottom: *aperture*, visible in view (a), defining the end of the interaction region for the laser and negative ions. *Ion deflector* that separates negative ions from neutralized atoms. *Faraday cup (FC)* reads the negative ion current. *Electron deflector* guides secondary electrons produced by the neutral particles hitting the detector glass plate. *Channel electron multiplier (CEM)* detects electrons guided from the detector glass plate by the *electron deflector*. *Detector box assembly* confines the indium tin oxide (ITO) coated glass plate.

Neutral atoms resulting from the photodetachment process are not affected by the electric field of the second deflector and thus continue to travel in the forward direction until impinging on an indium tin oxide (ITO) coated glass plate [31]. Secondary electrons emitted by the ITO under impact of the fast atoms are directed to a CEM (DeTech XP-2334) for detection. A mechanical drawing of this set-up is shown in figure 2. The entrance of the CEM is placed out of sight of the position where the atoms impinge on the coated glass plate. A curved electrode at a negative potential is used to deflect the electrons into the CEM. By switching the potential on this electrode, it is possible to allow/prevent secondary electrons from reaching the CEM. This feature is used to suppress the electrons emitted by the photoelectric effect when the laser pulse strikes the glass plate. The pulsed laser beam ensures that the atoms associated with the photodetachment process arrive in a well-defined time window, whilst the atoms originating from other detachment processes (e.g. residual gas interactions) are continuously distributed in time. Consequently, the non-photodetachment background can be easily measured.

Despite these efforts, the main source of background is still related to neutral atoms produced when the negative ions collide with the residual background gas. Ultra-high vacuum conditions are therefore required in the interaction region to achieve satisfactory experimental sensitivity. The GANDALPH apparatus is pumped with a $500\,\mathrm{l\,s^{-1}}$ turbo molecular pump. It was baked for 24 h at 140 °C prior to the experiment. Since the vacuum in the GLM beamline does not reach values below 2×10^{-6} mbar a differential pumping section was installed between GANDALPH and GLM. The entrance and exit of this chamber consisted of 10 mm diameter apertures. In this section two sets of deflection plates were placed for fine adjustment of the ion beam in the horizontal and vertical directions. The differential pumping section was

pumped with a $60\,\text{l}\,\text{s}^{-1}$ turbo molecular pump resulting in a pressure of 10^{-7} mbar. The base pressure in GANDALPH was 8×10^{-11} mbar, which increased to about 7×10^{-10} mbar when the valves enclosing the differential pumping section were opened.

2.4. Ion beam tuning

The initial beam tuning was performed using the stable iodine isotope ^{127}I available from the mass-marker capillary. A beam intensity of the order of 200 pA could be measured at the GLM FC upstream the GANDALPH setup. The maximum ion beam transport efficiency through the differential pumping section and GANDALPH was 25%.

2.5. Data acquisition

The signal from the CEM was fed into a two-channel gated photon counter (SR400, Stanford Research System). Two gates (corresponding to the channels *A, B*) with widths of 3.7 μs each were set in the acquisition system. Gate *A* with a delay of 1.9 μs registered events when the neutral atoms produced in the photodetachment process arrived at the detector. Gate *B* was delayed by 50 μs to detect collisionally produced neutral atoms. For each laser wavelength, set by the laser stabilizing software, the photon counter was set to accumulate for 10 cycles. In each cycle, the number of signal (channel *A*) background (channel *B*) counts and the laser wavelength measurements were recorded during 10 s (i.e. 10^5 laser pulses) and stored using the *LabVIEW* based RILIS data acquisition system [32]. The data acquisition was set up to operate asynchronous to the PSB. The requested equidistant proton pulses within the PSB pulse sharing super-cycle coupled with the relatively slow release (seconds) of iodine from the target matrix minimized fluctuations throughout the measurement.

3. Results

The ion beam intensity of the radioactive ^{128}I was too weak to be measured with the FC. Instead, the total ion rate was determined by turning off the electric field that deflects the ions, allowing them to continue with the neutral atoms to the coated glass plate. The secondary electrons created by the combined ion and atom beams were then measured by the CEM. This was performed before and after the photodetachment scan, yielding an average count-rate of 35 000 events per second.

Figure 3 shows the result of the LPT spectroscopy of ^{128}I$^-$ where the cross section of the photodetachment is plotted as a function of photon energy[8]. The data was recorded within a total of 39 min accumulation time in a co-propagating geometry. As described in section 2.5 the photon counter integrated the neutral particles detected during 10 s cycles. Each data point contains the background gate counts subtracted from the signal gate counts from the average of 10 acquisition cycles. Furthermore, the neutral particle count data is normalized by dividing each point with the averaged transmitted laser power during these 10 cycles to obtain a relative cross section for the photodetachment. The relative cross section, in figure 3, is scaled to the highest value of the data set. The error bars show the statistical uncertainty with a one sigma confidence interval. The solid line is a fit using the Wigner law [34] given by the expression

---

[8] Data from the wavelength meter was obtained in units of cm^{-1} and converted to eV using the 2014 CODATA [33] recommended values.
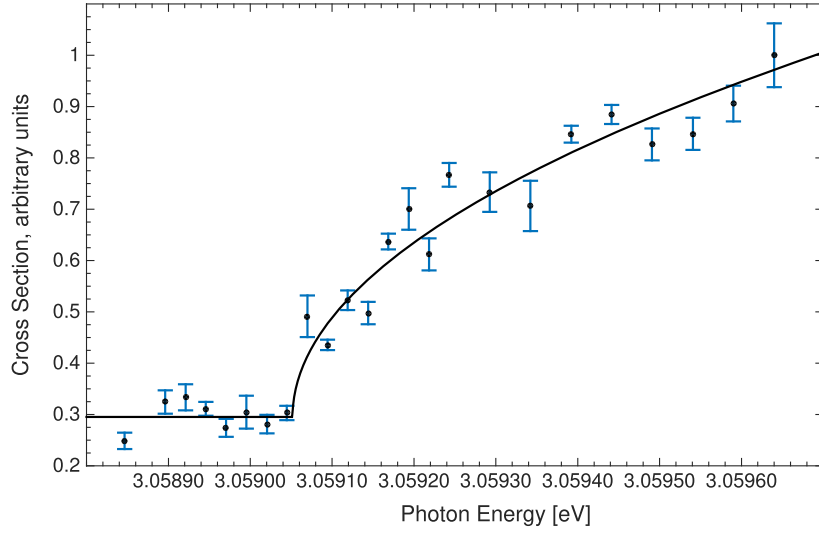
Figure 3. Normalized photodetachment cross section, in arbitrary units, of iodine $^{128}\mathrm{I}^-$ as a function of laser photon energy in electronvolts. The error bars represent the statistical uncertainty (one sigma). The energy scale has been corrected for the Doppler shift resulting from the high velocity of the negative ions. The Wigner threshold law fit is represented by the solid black line.

$$\sigma = \begin{cases} a + b(E_\gamma - E_{\mathrm{EA}})^{\ell+1/2} & \text{for } E_\gamma > E_{\mathrm{EA}}, \\ a & \text{for } E_\gamma < E_{\mathrm{EA}}. \end{cases} \tag{1}$$

Here a is a constant representing laser induced background[9] and b is a parameter describing the strength of the photodetachment process. E_γ is the photon energy and E_{EA} the EA. The cross section scales with the excess energy with an exponent $(\ell + 1/2)$, where ℓ is the angular momentum of the detached electron. The electron configuration of I^- is $5p^6\,^1\mathrm{S}_0$. The electron emitted in the photodetachment will therefore be a superposition of an s and a d wave. In the vicinity of the detachment threshold, however, the d-wave will be suppressed due to the centrifugal barrier. Hence, the angular momentum will be $\ell = 0$ for s-wave detachment, giving an exponent value of $1/2$ in the Wigner law.

In order to determine the EA of $^{128}\mathrm{I}^-$ from our measurement we need to correct the photon energy values of the co-propagating laser beam for the Doppler shift due to the ion velocity. The relativistic Doppler shift can be expressed in the form

$$f_{\mathrm{COM}} = \sqrt{\frac{c - v}{c + v}} f_{\mathrm{Lab}}, \tag{2}$$

where v is the ion velocity, c the speed of light and f_{COM} and f_{Lab} represent the laser frequency in the center-of-mass and laboratory frames, respectively. Solving for v one obtains the expression

---

[9] The laser induced background is either photodetachment of a contaminating negative ion with an EA that is smaller than that of iodine, or photo-electrons created from the laser impinging on the neutral particle detector glass plate. Due to the narrow photon energy scanning range, this background is assumed to be constant.

$$v = c \sqrt{\left(\frac{1 - R^2}{1 + R^2}\right)^2}, \qquad (3)$$

where

$$R = f_{\text{COM}} / f_{\text{Lab}}. \qquad (4)$$

In addition to the measurement of the ^{128}I$^-$ photodetachment threshold we recorded data for the threshold of the stable ^{127}I$^-$ isotope. We can determine f_{COM} using the known value of the EA of ^{127}I$^-$ [25], whereas f_{Lab} is the experimentally determined ^{127}I$^-$ photodetachment threshold. The velocity of the ions, and hence the kinetic energy of the ^{127}I$^-$ beam, can then be derived by using equations (3) and (4) and the well known relation between velocity and kinetic energy. The kinetic energy of the ion beam is independent of the mass due to identical acceleration voltage for both isotopes. Thus, by knowing the ion kinetic energy we can determine the velocity of the ^{128}I$^-$ beam. This velocity was used to correct the photon energy scale in figure 3 for the Doppler shift. The uncertainty in the determination of the kinetic energy of the beam is transferred to a systematic uncertainty in the ^{128}I EA of 13 μeV. The Wigner fit yields an EA of 3.059 052(25) eV, with a statistical uncertainty of 25 μeV with one sigma confidence interval. Adding the statistical and systematic uncertainty we obtain a final uncertainty of 38 μeV. Our final result of the EA of ^{128}I therefore becomes 3.059 052(38) eV.

4. Discussion

We have measured the EA of ^{128}I and obtained a value of 3.059 052(38) eV. The bandwidth of the laser used in this experiment is 10 GHz, which corresponds to 26 μeV. Hence the precision of the measurement is of the order of the laser bandwidth. The most precise determination of the EA of stable ^{127}I has been conducted by Peláez *et al* (using the photodetachment microscope technique), yielding 3.059 046 3(38) eV [25]. In an earlier experiment, Hanstorp and Gustavsson [35] used a set-up very similar to GANDALPH, obtaining a value of 3.059 038(10) eV for the EA of ^{127}I. As it can be seen, the measured EA value of the radioactive isotope ^{128}I coincides with the determinations of the stable isotope ^{127}I within their uncertainties.

These values should, in principle, differ due to the isotope shift effect, but the expected difference is smaller than the uncertainty in the current experiment. So far only a single isotope shift has been observed for iodine. This was performed by Engleman *et al* [36] who observed an ^{127,129}I isotope shift of 260 MHz in an optical transition. Isotope shifts for elements around $Z = 53$ typically are in the order of a few 100 MHz. For this size nuclei the volume shift is expected to be the dominating contributor to the isotope shift [37]. The normal mass shift between ^{127}I and ^{128}I is only 25 MHz or 0.1 μeV[10], and the specific mass shift is estimated to be of the same order of magnitude. Hence, we do not expect to be able to resolve the isotope shift between these two isotopes with the current experimental configuration.

In this experiment the two limiting factors for the accuracy are the bandwidth of the laser and the uncertainty in the Doppler shift due to the ion velocity. The latter can easily be excluded by performing the measurement in geometries involving both co- and counter-propagating laser beams. By taking the geometrical mean of the two measured threshold energies the Doppler shift contribution will be eliminated. The bandwidth of the laser can be reduced to about 1 GHz by adding an additional intra-cavity etalon into the Ti:Sa laser cavity

---

[10] Estimated from $\frac{\delta \text{EA}(A_L, A_H)}{\text{EA}(A_L)} \approx \frac{A_H - A_L}{1823 A_H A_L}$ [38], with A_L and A_H the mass numbers of the two iodine isotopes.

[39]. An even larger reduction can be obtained by using an injection-seeded Ti:Sa laser [40] with a bandwidth of only few 10 MHz. In this case, the isotope shift in the EAs of [127]I and [128]I should be resolvable.

As described in the introduction, one major goal of this project is to measure the EA of astatine. This quantity has not been experimentally determined, and theoretical predictions using different methods range between 2.11 and 3.18 eV, with the most recent calculation predicting a value of 2.412 eV [41]. The electron configurations of astatine and iodine are the same. Hence, the photodetachment of a $6p$ valence electron in astatine will give the same sharp onset as we observed for iodine. An experimental determination, even with an accuracy of just 1%, would be of great importance to benchmark quantum-chemical calculations. The data shown here for [128]I were recorded with an ion beam of about 35 000 ions per second and yielded an accuracy of 10^{-5} for data acquired in 39 min. Hence, a low resolution determination of the EA of astatine should be feasible within a reasonable accumulation time even if the ion beam intensity is limited to a few ions per second.

5. Conclusion

We have demonstrated the first photodetachment study of a negatively charged radioactive isotope. This result paves the way for measurements of the EAs of other radioactive elements such as astatine and polonium in the near future. In particular, the determination of the EA of astatine would be of great interest due to its importance in the radio-therapeutic method of TAT. Further on, measurements of the EAs of super-heavy elements could become feasible, although implementation at the corresponding production facilities will be technically challenging. The present experiment also demonstrates the new capabilities to study negatively charged radioactive ions at ISOLDE. A future project is planned to study the isotope shift of the EA across an isotopic chain of light elements (e.g. chlorine), in particular the specific mass shift that is caused by the electron correlation effect, which is particularly pronounced in negative ions [9, 42–44].

Acknowledgments

ORCID iDs

Sebastian Rothe ⬤ https://orcid.org/0000-0001-5727-7754
Yuan Liu ⬤ https://orcid.org/0000-0001-5903-3112

References

[1] Andersen T, Haugen H K and Hotop H 1999 *J. Phys. Chem. Ref. Data* **28** 1511
[2] Pegg D J 2004 *Rep. Prog. Phys.* **67** 857–905
[3] Wildt R 1939 *Astrophys. J.* http://adsabs.harvard.edu/full/1939ApJ....89..295W **89** 295–301
[4] McCarthy M C, Gottlieb C A, Gupta H and Thaddeus P 2006 *Astrophys. J. Lett.* **652** L141
[5] Kar S and Ho Y K 2005 *New J. Phys.* **7** 141
[6] Litherland A E 1980 *Annu. Rev. Nucl. Part. Sci.* **30** 437–73
[7] Simonin A *et al* 2015 *Nucl. Fusion* **55** 123020
[8] Chaibi W, Peláez R J, Blondel C, Drag C and Delsart C 2010 *Eur. Phys. J.* D **58** 29–37
[9] Berzinsh U, Gustafsson M, Hanstorp D, Klinkmüller A, Ljungblad U and Mårtensson-Pendrill A M 1995 *Phys. Rev. A* **51** 231–8
[10] Asimov I 1953 *J. Chem. Educ.* **30** 616
[11] Wilbur D 2008 *Curr. Radiopharm.* **1** 144–76
[12] Vaidyanathan G and Zalutsky M 2008 *Curr. Radiopharm.* **1** 177–96
[13] Sergentu D C, David G, Montavon G, Maurice R and Galland N 2016 *J. Comput. Chem.* **37** 1345–54
[14] Champion J, Alliot C, Renault E, Mokili B M, Cherel M, Galland N and Montavon G 2010 *J. Phys. Chem. A* **114** 576–82
[15] Champion J, Seydou M, Sabatié-Gogova A, Renault E, Montavon G and Galland N 2011 *Phys. Chem. Chem. Phys.* **13** 14984
[16] Champion J, Sabatié-Gogova A, Bassal F, Ayed T, Alliot C, Galland N and Montavon G 2013 *J. Phys. Chem. A* **117** 1983–90
[17] Pauling L 1932 *J. Am. Chem. Soc.* **54** 3570–82
[18] Rothe S *et al* 2013 *Nat. Commun.* **4** 1835
[19] Kugler E 2000 *Hyperfine Interact.* **129** 23–42
[20] Kofoed-Hansen O and Nielsen K O 1951 *Mat.-Fys. Medd. K. Dan. Vidensk. Selsk.* **26**
[21] Kluge H J 1986 *ISOLDE Users' Guide* (Geneva: CERN)
[22] Burke D G *et al* 1989 *Z. Phys. A* **333** 131–5
[23] Vosicki B, Björnstad T, Carraz L, Heinemeier J and Ravn H 1981 *Nucl. Instrum. Methods Phys. Res.* **186** 307–13
[24] Stora T, Wilfinger R, Bouquerel E, Catherall R, Eller M, Lettry J and Menna M 2006 *First negative halogen beams produced at PSBooster-ISOLDE* EURISOL-03-22-2006-0011 CERN https://cds.cern.ch/record/1356484
[25] Peláez R J, Blondel C, Delsart C and Drag C 2009 *J. Phys. B: At. Mol. Opt. Phys.* **42** 125001
[26] Diehl C, Wendt K, Lindahl A O, Andersson P and Hanstorp D 2011 *Rev. Sci. Instrum.* **82** 053302
[27] Hanstorp D 1995 *Nucl. Instrum. Methods Phys. Res. B* **100** 165–75
[28] Andersson P, Lindahl A O, Alfredsson C, Rogström L, Diehl C, Pegg D J and Hanstorp D 2007 *J. Phys. B: At. Mol. Opt. Phys.* **40** 4097
[29] Rothe S, Marsh B A, Mattolat C, Fedosseev V N and Wendt K 2011 *J. Phys.: Conf. Ser.* **312** 052020
[30] Rothe S, Goodacre T D, Fedorov D, Fedosseev V, Marsh B, Molkanov P, Rossel R, Seliverstov M, Veinhard M and Wendt K 2016 *Nucl. Instrum. Methods Phys. Res. B* **376** 91
[31] Hanstorp D 1992 *Meas. Sci. Technol.* **3** 523–7
[32] Rossel R *et al* 2013 *Nucl. Instrum. Methods B* **317** 557–60
[33] Mohr P J, Newell D B and Taylor B N 2016 *Rev. Mod. Phys.* **88** 035009
[34] Wigner E P 1948 *Phys. Rev.* **73** 1002–9
[35] Hanstorp D and Gustafsson M 1992 *J. Phys. B: At. Mol. Opt. Phys.* **25** 1773–83
[36] Engleman R, Keller R and Palmer B 1980 *Appl. Opt.* **19** 2767–70
[37] King W 1984 *Physics of Atoms and Molecules* (New York: Plenum)
[38] Drake G 2006 *Springer Handbook of Atomic, Molecular, and Optical Physics* (Berlin: Springer)
[39] Rothe S, Fedosseev V, Kron T, Marsh B, Rossel R and Wendt K 2013 *Nucl. Instrum. Methods Phys. Res. B* **317 Part B** 561–4
[40] Kessler T, Tomita H, Mattolat C, Raeder S and Wendt K 2008 *Laser Phys.* **18** 842
[41] Borschevsky A, Pašteka L F, Pershina V, Eliav E and Kaldor U 2015 *Phys. Rev. A* **91** 020501
[42] Godefroid M and Fischer C 1999 *Phys. Rev. A* **60** R2637–40
[43] Jönsson P and Godefroid M 2000 *Mol. Phys.* **98** 1141–9
[44] Carette T and Godefroid M R 2014 *Phys. Rev. A* **89** 1–8